This is a preprint, the final version is subject to change, of the American Mineralogist (MSA)
Cite as Authors (Year) Title. American Mineralogist, in press.
DOI: https://doi.org/10.2138/am-2019-6802

**Revision 1**

# Fast diffusion path for water in silica glass

**Minami Kuroda[1], Shogo Tachibana[1, 2], Naoya Sakamoto[3], and Hisayoshi Yurimoto[1, 3, 4]**

[1]Departmant of Natural History Sciences, Hokkaido University, N10W8 Sapporo 060-0810, Japan.

[2]UTokyo Organization for Planetary and Space Science, University of Tokyo, 7-3-1 Hongo 113-0033, Japan.

[3]Isotop Imaging Laboratory, Hokkaido University, N21W10 Sapporo 001-0021, Japan.

[4]Institute of Space and Astronautical Science, JAXA, 3-1-1 Yoshinodai, Sagamihara 252-5120, Japan.

Corresponding author: Minami Kuroda (minami@ep.sci.hokudai.ac.jp)

This is a preprint, the final version is subject to change, of the American Mineralogist (MSA)
Cite as Authors (Year) Title. American Mineralogist, in press.
DOI: https://doi.org/10.2138/am-2019-6802

## Abstract

Diffusion experiments of $^2H_2O$ at 900-750°C and water vapor pressure of 50 bar found more than one-order of magnitude faster diffusion of water in $SiO_2$ glass than that reported previously. The fast diffusion profile of water was observed as an extended tail of the normal water diffusion profile by a line scan analysis with SIMS, and it can be fitted with a diffusion model with a constant diffusivity. The obtained fast diffusion coefficient suggests that the diffusion species responsible for the fast diffusion is not molecular hydrogen but molecular water. The diffusivity and activation energy for the fast water diffusion can be explained by the correlation between diffusivities of noble gases in silica glass and their sizes. Because noble gases diffuse through free volume in the glass structure, we conclude that molecular water can also diffuse through the free volume. The abundance of free volume in the silica glass structure estimated previously is higher than that of $^2H$ observed in the fast diffusion in this study, suggesting that the free volume were not fully occupied by $^2H$ under the present experimental condition. This implies that the contribution of the fast water diffusion to the total water transport in volcanic glass becomes larger under higher water vapor pressure conditions.

29 Key words: water, silica glass, SIMS, diffusion pathway, free volume

30

This is a preprint, the final version is subject to change, of the American Mineralogist (MSA)
Cite as Authors (Year) Title. American Mineralogist, in press.
DOI: https://doi.org/10.2138/am-2019-6802

## INTRODUCTION

Water inside the Earth changes physical and chemical properties of rocks, minerals, and magma. Water circulates into the mantle through subduction zones and back to the surface through arc volcanism. The arc volcanism is affected by water in magma because water changes the physical and chemical properties of magma. For instance, water influences eruption styles through changing magma ascent rates via its influence on bubble nucleation, bubble growth, and degassing (e.g., Sparks, 1978; Rutherford, 2008). Bubble growth in magma is controlled by viscous relaxation and water diffusion, the relative influence of which depends on magma properties such as temperature, pressure, and chemical compositions.

Water diffusion in magma is therefore one of the important basic parameters to control water degassing from magmas. Water diffusion in various silicate glasses, as an analog of silicate melts, has been intensively studied (e.g., Zhang et al., 2007 and references therein). Although the dependences of water diffusion on temperature, water concentration, and pressure have been obtained and formulated, water diffusion in silicate glasses is not yet fully understood as an atomistic-scale process. Kuroda et al. (2018) performed water diffusion experiments in silica glass,

and proposed a water diffusion model, where water molecules diffuse through pathways formed by hydroxyls. They also showed that the model is applicable to the water diffusion in various silicate glasses to explain the concentration dependence of water diffusion in rhyolite and basalt glasses.

Here we report a new diffusion pathway of water molecules in silica glass, through which water can be transported at a rate of one-order of magnitude faster than that previously reported values in similar conditions as Kuroda et al. (2018). We discuss the mechanism of water molecule diffusion through the fast pathway and its potential contribution to the water transport in silicate glasses.

## EXPERIMENTAL AND ANALYTICAL METHODS

Diffusion experiments were performed using the same protocol as in Kuroda et al. (2018). An optical silica glass plate (5 mm × 3 mm × 2 mm; SIGMA KOKI CO.) was flame-sealed in a silica glass tube (3.5 mm and 4.7 mm in inner and outer diameters, and 80 mm in length) with deuterated water ($^2H_2O$) (7.10-8.17 μL) under atmospheric pressure. The sealed glass tubes were heated in a box furnace at temperatures of 900, 850, 800 and 750 °C for different durations (Table

1). The $^{2}H_2O$ vapor pressure inside the glass tube was controlled to be 50 bar by complete evaporation of deuterated water.

Polished cross sections of the run products were prepared for measurements of concentration profiles of $^{1}H$, $^{2}H$, and $^{30}Si$ along the diffusion direction from the glass surface with a secondary ion mass spectrometer (SIMS; Cameca ims-6f) at Hokkaido University. A 15-20 nA Cs+ primary beam was focused to form a 20-25-μm spot on the sample, and negatively charged secondary ions of $^{1}H$, $^{2}H$, and $^{30}Si$ were counted by an electron multiplier for 2, 10, and 1 seconds, respectively, with a 5 μm step. A normal electron flood gun was used for charge compensation. A field aperture was used to permit transmission of ions from the central area of 10 μm in diameter of the sputtered region to minimize the hydrogen signals from absorbed water on the sample surface. A few profiles (mostly three) were obtained for each sample to assess the analytical reproducibility. A starting material glass sample was also measured as a reference with the same analytical condition. The position of the glass surface was determined as being the point from which $^{30}Si$ counts became constant.

This is a preprint, the final version is subject to change, of the American Mineralogist (MSA)
Cite as Authors (Year) Title. American Mineralogist, in press.
DOI: https://doi.org/10.2138/am-2019-6802

## RESULTS

Diffusion profiles of $^{2}H$ in samples heated at 900 °C for 1, 3, and 20 hours are compared in Fig. 1. The $^{2}H$ intensity decreases rapidly from rim to core of the sample with diffusion distances of about 50, 100, and 250 μm for the samples heated for 1, 3, and 20 hours, respectively. This is consistent with the diffusion experiments with $^{1}H_2O$ (Kuroda et al., 2018), and the profile shape can be explained by water concentration-dependent diffusion in silica glass (Kuroda et al., 2018), of which detail is discussed below.

It is found that the tail of deuterium profile extends further into the deep region of the sample, where the $^{2}H$ ion intensity is higher than the original value in the starting material ($^{2}H/^{30}Si < 2 \times 10^{-7}$) (Fig. 1). Comparison between the concentration profiles heated at 900°C for 1 and 3 hours clearly shows that $^{2}H$ migrated into the deeper region of the glass with time (Fig. 1). The $^{2}H$ finally seems to have an almost homogeneous distribution inside the glass after 20-hour heating (Fig. 1). This observation clearly shows that a small fraction of deuterium-bearing species migrates at a faster diffusion rate than the dominant fraction that diffuses as the concentration dependent

profile. This newly-observed fast diffusion profile was also confirmed in samples heated at 850, 800, and 750 °C (Fig. 2).

## DISCUSSION

### Profile fitting

The profiles of $^{2}H/^{30}Si$ in the run products are used to discuss the $^{2}H_2O$ diffusion because it has a linear relation to the water concentration (Kuroda et al., 2018). The $^{2}H/^{30}Si$ profiles, normalized to the ratio at the glass surface, are shown in Fig. 2. The concentration-dependent diffusion profiles can be explained by the water diffusion model in silica glass (Kuroda et al., 2018), where molecular water is proposed to diffuse through the pathway formed by hydroxyls (-OH). The model attributes the strong water concentration dependence for water diffusion in silica glass to the limited number of diffusion pathways. If water molecules ($H_2O_m$) favor a pathway formed by cuting Si-O-Si bonds to diffuse in the polymerized silica glass network, water molecules themselves should form the pathways through the hydroxyl formation reaction ($\boldsymbol{H_2O_m + O \leftrightarrow 2OH}$). On the other hand, such pathways preexist in silicate glasses due to the presence of network modifier cations such as $Na^+$ and $K^+$ that cut the glass network. This difference results in the

stronger water concentration dependence for water diffusion in silica glass than in silicate glasses because the number of diffusion pathways in silica glass depends on water concentration (Kuroda et al., 2018).

The total water diffusivity ($\boldsymbol{D_{H_2O_t}}$) in silica glass through the pathways formed by hydroxyls ('normal diffusion' hereafter) is given by

$$\boldsymbol{D_{H_2O_t}} = \frac{\boldsymbol{D^*K}}{\boldsymbol{8}}\left(\left(\boldsymbol{1}+\frac{\boldsymbol{16X_{H_2O_t}}}{\boldsymbol{K}}\right)^{\frac{\boldsymbol{1}}{\boldsymbol{2}}}-\boldsymbol{1}\right)\left(\boldsymbol{1}-\left(\boldsymbol{1}+\frac{\boldsymbol{16X_{H_2O_t}}}{\boldsymbol{K}}\right)^{-\frac{\boldsymbol{1}}{\boldsymbol{2}}}\right), \quad (1)$$

where $X_i$ is the molar fraction of species $i$, $D^*$ is a concentration independent term and $K$ is an equilibrium constant of the hydroxyl formation reaction (Kuroda et al., 2018). The water diffusion profiles fitted with the diffusion coefficient of Eq. (1) are shown as dotted curved in Fig. 2. The diffusivities for normal diffusion at the glass surface are about (5-0.8) $\times 10^{-13}$ m$^2$/s in the present experimental conditions, and decreases with decreasing $\boldsymbol{X_{H_2O_t}}$ in roughly proportion to $\boldsymbol{X^2_{H_2O_t}}$ (Kuroda et al., 2018).

The extended tails of the diffusion profiles ('fast diffusion' hereafter) cannot be explained by the normal diffusion, while they can be fitted by a one-dimensional, semi-infinite diffusion

This is a preprint, the final version is subject to change, of the American Mineralogist (MSA)
Cite as Authors (Year) Title. American Mineralogist, in press.
DOI: https://doi.org/10.2138/am-2019-6802

model with a fixed surface concentration and a constant diffusion coefficient (Crank, 1975) assuming that the fast diffusion is independent of the normal diffusion (Fig. 2):

$$\boldsymbol{R(x) = (R_s - R_0)\left[1 - erf\left(\frac{x}{2\sqrt{Dt}}\right)\right] + R_0}, \quad (2)$$

where $x$ is the distance from the glass surface, $R(x)$ is the normalized $^{2}H/^{30}Si$ at $x$, $R_s$ is the normalized $^{2}H/^{30}Si$ at the glass surface for fast diffusion, $R_0$ is the background $^{2}H/^{30}Si$ relative to $R_s$, respectively. The fitting curves were obtained for the first ~100-μm of the tails (Fig. 2) because the $^{2}H$ intensities in the deeper region became comparable to the detection limit. The obtained diffusion coefficients of fast diffusion (Table 1) are about one-order of magnitude larger than those of normal water diffusion at the glass surface at all temperatures. They are more than one order of magnitude larger than the normal diffusion coefficients inside the glass ((5-0.8) $\times 10^{-13}$ $m^2/s$ at the glass surface under the present experimental conditions), where the total water concentration is lower than at the surface.

The diffusion model with a constant diffusion coefficient gives $R_s$ of (2–6) $\times 10^{-4}$ at all the temperatures. Although the estimated $R_s$ has a large uncertainty, it is comparable to the

133 homogeneous *R(x)* within the samples heated for 20 hours ((4–12) $\times 10^{-4}$). This suggests that the
134 assumption of the fixed surface concentration in Eq. (2) is valid.

135

136 **Species and path for fast diffusion of water in silica glass**

137 Mean values of the fast diffusion coefficients at different temperatures, obtained from
138 multiple-line profiles of a single sample, are summarized in Table 1. The Arrhenius plot of the fast
139 diffusion coefficient gives an activation energy of 80.5 ± 40.5 kJ/mol and a pre-exponential factor
140 of $6.1 \times 10^{-9}$ $m^2/s$ (Fig. 3).

141 The obtained diffusion coefficient at 900-750°C (Table 1) is two orders of magnitude
142 smaller than that of $H_2$ in the same temperature range (Lou et al., 2003), and its activation energy is
143 twice as large as that of $H_2$ diffusion in silica glass (Lou et al., 2003). Therefore $H_2$ is unlikely to be
144 a diffusing species for the fast diffusion observed in this study.

145 The activation energy of ~80.5 kJ/mol is similar to that of the normal diffusion of water in
146 silica glass (e.g., Kuroda et al., 2018; Wakabayashi and Tomozawa, 1989). This indicates that the

147 main diffusion species for fast diffusion is molecular water and that water molecules jump within
148 the glass structure with a similar energetic barrier (Kuroda et al., 2108).

149 The similar energetic barrier for normal and fast diffusion suggests that the difference in
150 diffusivity should be attributed to factors related to the pre-exponential term for diffusion such as a
151 frequency factor and a diffusion pathway. Here we propose that a small fraction of water molecules
152 diffuse through the pathways connecting free volume (Fig. 4) without reacting with the silica glass
153 structure to form hydroxyls. The free volume is the intrinsic gap formed within the polymerized
154 network (e.g., Cohen and Turnbull, 1959; Vrentas and Duda, 1977), and it has been proposed that
155 noble gases diffuse through the free volume in the network structure of silica and silicate glasses
156 (e.g., Behrens, 2010; Amalberti et al., 2016) (Fig. 4(a)). In the free-volume diffusion model, the
157 free volumes are connected by "doorways" of an average radius $r_0$. The activation energy for the
158 diffusion may be given as the energy required to deform the glass network large enough to allow an
159 atom to pass from one side to another. For instance, the following expression has been proposed for
160 the relationship between the activation energy for diffusion and the atomic radius ($r$) for noble
161 gases;

$$E_a = 8\pi G r_0 (r - r_0)^2, \quad (3)$$

where $G$ represents a shear modulus of the glass. $G$ and $r_0$ for silica glass are estimated to be 305 kbar and 1.1 Å, respectively (Anderson and Stuart, 1954).

The obtained diffusivity and the activation energy for the fast diffusion of water molecules are compared with those of noble gas diffusion in silica glass (Swets et al., 1961 for He; Wortmann and Shakelford, 1990 for Ne; Carroll and Stolper, 1991 for Ar; Roselieb et al., 1995 for Kr and Xe) (Fig. 4(b)). The radii of noble gasses and molecular water are taken from Zhang and Xu (1995), where molecule radii were obtained by treating the noble gas atoms as ions of zero oxidation states. The free volume diffusion of noble gases in silicate glasses shows the non-Arrhenius relation at temperatures close to the glass transition temperature (e.g., Amalberti et al., 2016) most likely because of the structural change of the glass network. However, the effect of the structural change on the free volume diffusion is negligibly small in this study because the temperature range discussed here is much below the glass transition temperature of silica glass (~1163°C; Calculated with Deubener et al., 2003), where the free volume diffusion of noble gases show a simple Arrhenius relation.

177 The activation energies of noble gas diffusion in silica glass show a clear relation with the
178 atomic radius, and they increase with increasing the atomic size (Fig. 4(b)). Although the reported
179 activation energies of noble gases are not well fit by the relation with Eq. (3), the activation energy
180 for the fast diffusion of molecular water lies on the same trend of noble gas diffusion in silica glass.
181 Moreover, the pre-exponential factor for the fast water diffusion ($6.1 \times 10^{-9}$ $m^2/s$) fits within the
182 range of those for noble gas diffusion in silica glass ($7 \times 10^{-8}$ and $2 \times 10^{-9}$ $m^2/s$ for He and Kr,
183 respectively) (Fig. 4 (b)). These similarities of activation energy and pre-exponential factors
184 suggest that fast diffusion of molecular water is also governed by molecular jumps between
185 connecting free volume in the silica glass structure.

186

187 **Implications**

188 We found that there are, at least, two different pathways for water diffusion in silica glass
189 (normal diffusion through pathways created by the hydroxyl formation reaction and fast diffusion
190 through connected free volume). We here discuss the possible
191 contribution of the fast water diffusion to water transport in silica glass.

192 The amount of water transported by the fast diffusion can be estimated by integrating the
193 fast diffusion profiles, and it is ~0.5 % of the amount of water transported by normal diffusion at
194 900 °C. The surface concentration of water for the fast diffusion path is 3-4 orders of magnitude
195 smaller than the total water concentration at the surface (Fig. 2). Because the surface concentration
196 of dissolved water under the present experimental conditions is ~0.3 mol% (Kuroda et al., 2018),
197 the surface concentration of fast diffusion is estimated to range from a few ppm to several hundred
198 ppb. The estimated surface concentration of fast diffusion is likely to represent the water
199 concentration in connected free volume at the surface, and is much smaller than the concentration
200 of free volume in silica glass that was estimated from the solubility of Ar (~0.2 mol%; Shacklford,
201 1999). This implies that the free volumes were not fully occupied by water molecules at water
202 vapor pressure of 50 bar in the present experiments. We note that water concentration in the
203 starting silica glass is 10 ppm, well below the free volume concentration, such that it should not
204 affect the fast diffusion of $^2H_2O$ even if the initial water was present in glass' free volumes.

205 The solubility of molecular water in the fast diffusion path is expected to increase with
206 increasing the water vapor pressure until free volume saturation. The concentration of molecular

water occupying the free volume is likely to increase linearly with the water vapor pressure following the Henry's law as noble gases, while the solubility of water in the bulk glass depends on the square root of water vapor pressure (<~200 MPa) (e.g., Zhang et al., 2007).

We emphasize that more experimental work is clearly needed to determine the pressure dependence of water solubility in free volume, but the finding in this study may imply that the contribution of fast water diffusion to water transport in silica glass may become larger under higher water vapor pressures. Especially, its contribution could be significant for water diffusion occurring within a timescale shorter than a few hours as seen in this study, which the timescale of magma ascent for explosive eruption (e.g., Lloyd et al., 2014). The fast water diffusion might affect the nucleation and growth of bubbles in ascending magma.

## Acknowledgments

This work was supported by Ministry of Education, Sports, Science and Technology Kakenhi Grant. Constructive reviews from C.L. Losq and J. Amalberti are greatly appreciated.

## References

Amalberti, J., Burnard, P., Laporte, D., Tissandier, L., and Neuville, D.R. (2016) Multidiffusion mechanisms for noble gases (He, Ne, Ar) in silicate glasses and melts in the transition temperature domain: Implications for glass polymerization. Geochemica et Cosmochemica Acta, 172, 107-126.

Anderson, O.L., and Stuart, D.A. (1954) Calculation of activation energy of ionic conductivity in silica glasses by classical methods. Journal of the American Ceramic Society, 37, 573-580.

Behrens, H. (2010) Noble gas diffusion in silicate glasses and melts. Reviews in Mineralogy and Geochemistry, 72, 227-267.

Behrens, H., and Zhang, Y. (2001) Ar diffusion in hydrous silicic melts: implications for volatile diffusion mechanisms and fractionation. Earth and Planetary Science Letters, 192, 363-376.

233 Carroll, M.R., and Stolper, E.M. (1991) Argon solubility and diffusion in silica glass: Implications
234 for the solution behavior of molecular gases. Geochemica et Cosmochemica Acta, 55,
235 211-225.

236 Cohen, M.H., and Turnbull, D. (1959) Molecular transport in liquids and glasses. The Journal of
237 Chemical Physics, 31, 1164-1169.

238 Crank, J. (1975) The Mathematics of Diffusion Second Edition, 414 p. Oxford University Press,
239 Oxford.

240 Deubener, J., Müller, R., Behrens, H., and Heide, G. (2003) Water and the glass transition
241 temperature of silicate melts. Journal of Non-Crystalline Solids, 330, 268-273.

242 Kuroda, M., Tachibana, S., Sakamoto, N., Okumura, S., Nakamura, M., and Yurimoto, H. (2018)
243 Water diffusion in silica glass through pathways formed by hydroxyls. American
244 Mineralogist, 103, 412-417.

245 Lloyd, A.S., Euprecht, P., Hauri, E.H., Rose, W., Gonnermann, H.M., and Plank, T. (2014)
246 NanoSIMS results from olivine-hosted melt embayments: Magma ascent rete during
247 explosive basaltic eruptions, 283, 1-18

248 Lou, V., Sato, R., and Tomozawa. M. (2003) Hydrogen diffusion in fused silica at high
249 temperatures. Journal of Non-Crystalline Solids, 315, 13-19.

250 Ni, H., Hui, H., and Steinle-Neumann, G. (2015) Transport properties of silicate melts. Review of
251 Geophysics, 53, 715-744.

252 Roselieb, K., Rammensee, W., Büttner, H., and Rosenhaure, M. (1995) Diffusion of noble gases in
253 melts of the system $SiO_2$-$NaAlSi_2O_6$. Chemical Geology, 120, 1-13.

254 Rutherford, M.J. (2008) Magma Ascent Rates, Reviews in Mineralogy and Geochemistry, 69,
255 241-271.

256 Shackelford, J.F. (1999) Gas solubility in glasses – principles and structural implications. Journal
257 of Non-Crystalline Solids, 231-241.

258 Sparks, R.S.J. (1978) The dynamics od bubble formation and growth in magmas: a review and
259 analysis, Journal of Volcanology and Geothermal Research, 3, 1-37.

260 Swets, D.E., Lee, R.W., and Frank, R.C. (1961) Diffusion coefficients of helium in fused quarts,
261 The Journal of Chemical Physics, 34, 17-22.

262 Vrentas, J.S., and Duda, J.L. (1977) Diffusion in polymer – solvent systems. i. reexamination of the
263 free-volume theory. Journal of Polymer Sciene, 15, 403-416.

264 Wakabayashi, H., and Tomozawa, M. (1989) Diffusion of water into silica glass at low
265 temperature. Journal of the American Ceramic Society, 72, 1850-1855.

266 Wortman, R.S., and Shackelford, J.F. (1990) Gas transport in vitreous silica fibers. Journal of
267 Non-Crystalline Solids, 125, 280-286.

268 Zhang, Y., and Xu, Z. (1995) Atomic radii of noble gas elements in condensed phases. American
269 Mineralogist, 80, 670-675.

270 Zhang, Y., Xu, Z., Zhu, M., and Wang, H. (2007) Silicate melt properties and volcanic resutions.
271 Reviews of Geophysics, 45, RG4004.

272

273

**Figure 1.** Typical ion intensity profiles of $^{1}H$, $^{2}H$ and $^{30}Si$ (900 °C for 1, 3, and 20 hours). $^{1}H$ signals inside the glass are from backgrounds.

**Figure 2.** Typical diffusion profiles of $^{2}H$, shown as $^{2}H/^{30}Si$ normalized to that at the surface, in silica glass at 900, 850, 800, and 750 °C and a water pressure of 50 bar. The "normal water diffusion" profiles are fitted with the concentration-dependent water diffusion model (dashed curves) (Kuroda et al., 2018), and the "fast water diffusion" profiles are fitted with the constant-independent water diffusion model (solid curves). All $^{2}H/^{30}Si$ ratios are normalized to the $^{2}H/^{30}Si$ at the glass surface. For fitting of the "normal water diffusion" profiles, $D^*$, $K$, and the surface water concentration were taken from Kuroda et al. (2018), where diffusion experiments were performed under the same condition as in the present study (850-650 °C). $K$ and $D^*$ for 900 °C were obtained by the extrapolation of those in Kuroda et al. (2018), and the surface concentration was assumed to be the same as at 850 °C. The surface water concentration of all run products in this study is estimated to be about ~0.3 mol% based on the experiments by Kuroda et al. (2018).

**Figure 3.** The Arrhenius plot of the diffusion coefficient of fast water diffusion (eq. 2). The line is a fit to the data. Error bars represent 2-sigma standard deviations of the diffusion coefficients evaluated from multiple diffusion profiles.

**Figure 4. (a)** Schematic illustration of the diffusion mechanism through connected free volume. **(b)** Comparisons of activation energy for fast water diffusion and noble gas diffusion in silica glass (left) and of temperature dependence of diffusion coefficients (right). Activation energies and diffusion coefficients of noble gases in silica glass are taken from Swets et al. (1961) for He, Wortmann and Shakelford (1990) for Ne, Carroll and Stolper (1991) for Ar, and Roselieb et al. (1995) for Kr and Xe. Radii of noble gases and water molecule are taken from Zhang and Xu (1995). The relation between the activation energy and the radius of the diffusing species, obtained with Eq. (3) with $G$ = 305 kbar and $r_0$ = 1.1 Å (Anderson and Stuart, 1954), is also shown.

300 **Table 1.** Experimental conditions and diffusion coefficients of fast water diffusion in silica glass.
301 Errors are 2-sigma standard deviations of the diffusion coefficients evaluated from multiple
302 diffusion profiles. The samples heated for 1 hour and 20 hours were not used to determine the
303 diffusion coefficients because of their short diffusion profiles and homogeneous $^{2}H$ distributions,
304 respectively.

305

| Run No. | T(°C) | t (hours) | $D$ ($m^2/s$) |
|---|---|---|---|
| 900-1 | 900 | 3 | 1.61 (±0.42) x$10^{-12}$ |
| 900-2 | 900 | 3 | 1.87 (±0.60) x$10^{-12}$ |
| 900-3 | 900 | 20 | - |
| 900-4 | 900 | 1 | - |
| 850-1 | 850 | 3 | 0.92 (±0.25) x$10^{-12}$ |
| 850-2 | 850 | 3 | 1.58 (±0.41) x$10^{-12}$ |
| 800-1 | 800 | 3 | 0.42 (±0.14) x$10^{-12}$ |
| 800-2 | 800 | 3 | 0.66 (±0.11) x$10^{-12}$ |
| 800-3 | 800 | 3 | 0.57 (±0.37) x$10^{-12}$ |
| 750-1 | 750 | 3 | 0.67 (±0.17) x$10^{-12}$ |
| 750-2 | 750 | 3 | 0.55 (±0.08) x$10^{-12}$ |
| 750-3 | 750 | 20 | - |

306

307

This is a preprint, the final version is subject to change, of the American Mineralogist (MSA)
Cite as Authors (Year) Title. American Mineralogist, in press.
DOI: https://doi.org/10.2138/am-2019-6802

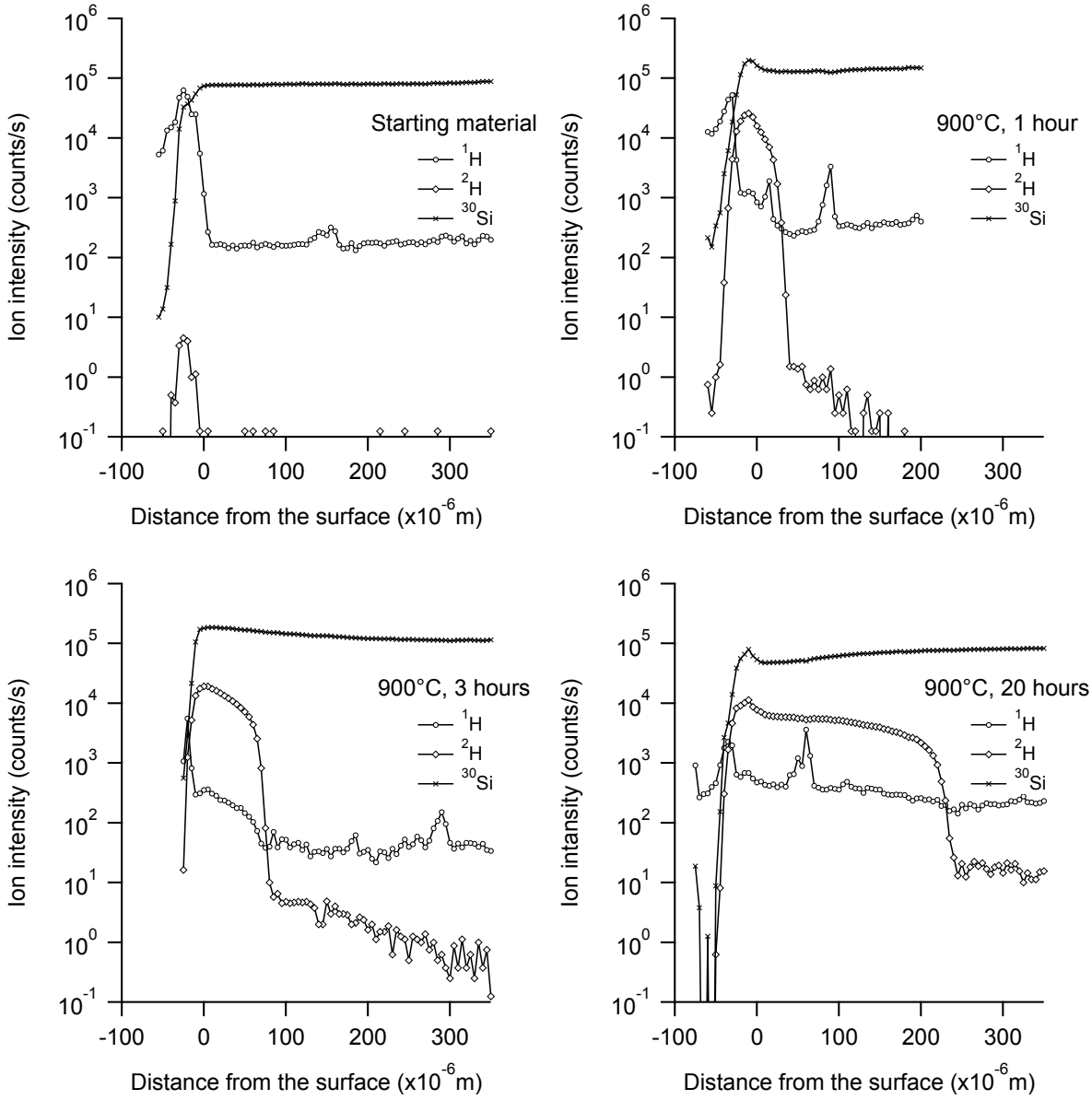


**Figure 1**

This is a preprint, the final version is subject to change, of the American Mineralogist (MSA)
Cite as Authors (Year) Title. American Mineralogist, in press.
DOI: https://doi.org/10.2138/am-2019-6802

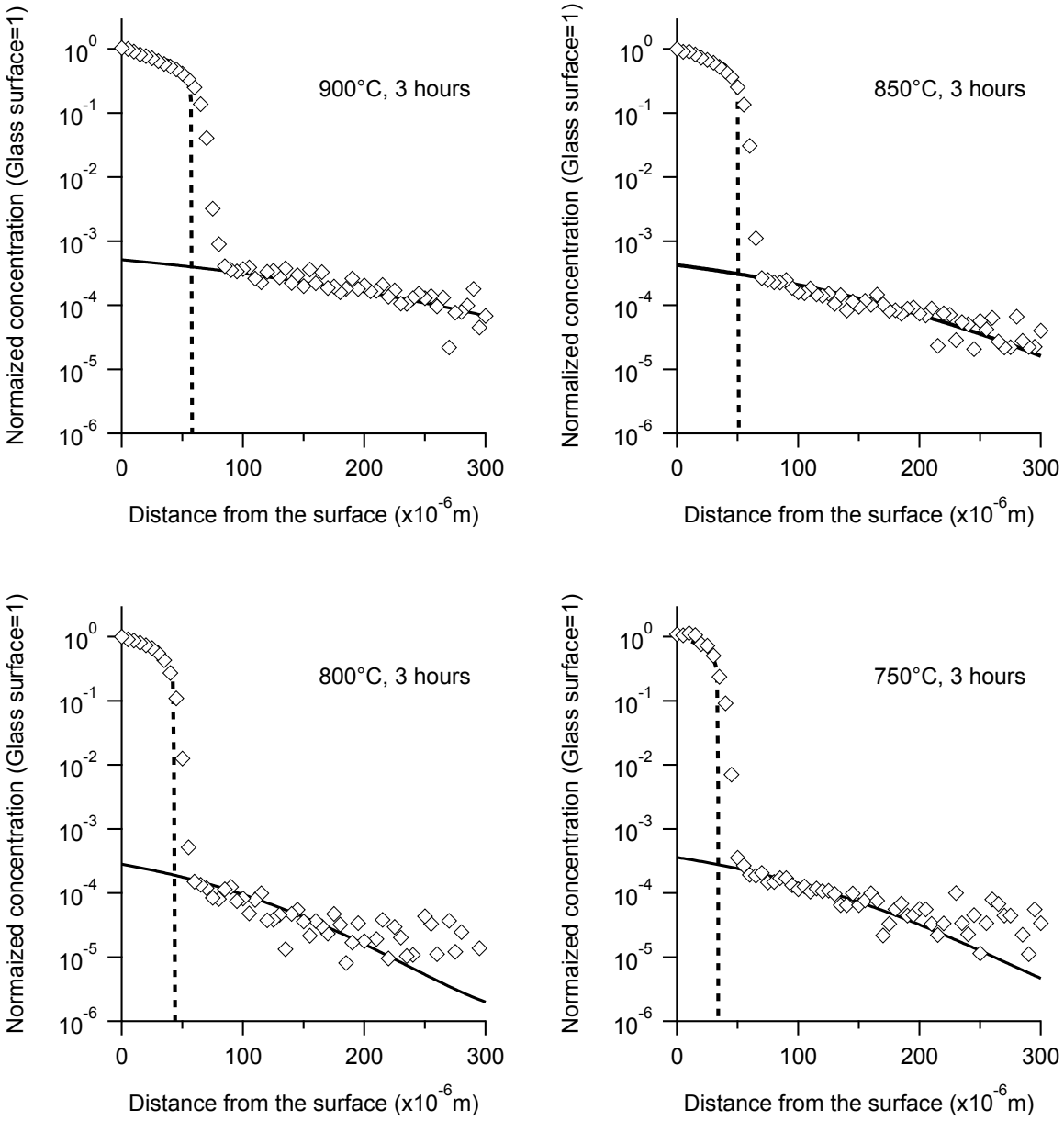


**Figure 2**

This is a preprint, the final version is subject to change, of the American Mineralogist (MSA)
Cite as Authors (Year) Title. American Mineralogist, in press.
DOI: https://doi.org/10.2138/am-2019-6802

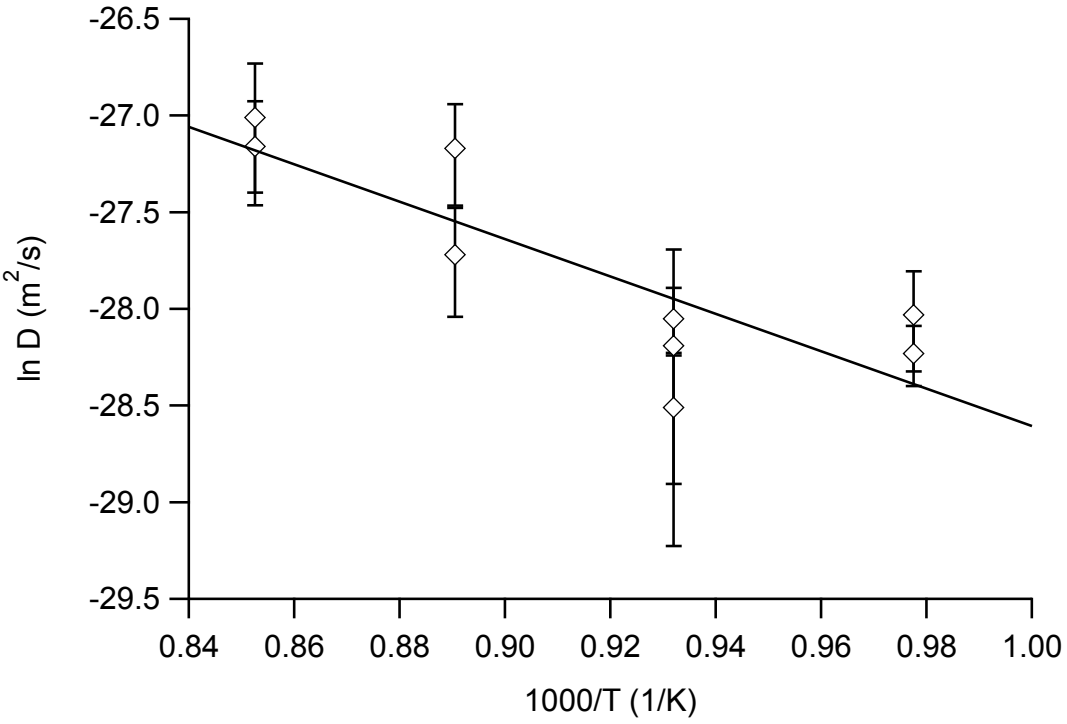


**Figure 3**

This is a preprint, the final version is subject to change, of the American Mineralogist (MSA)
Cite as Authors (Year) Title. American Mineralogist, in press.
DOI: https://doi.org/10.2138/am-2019-6802

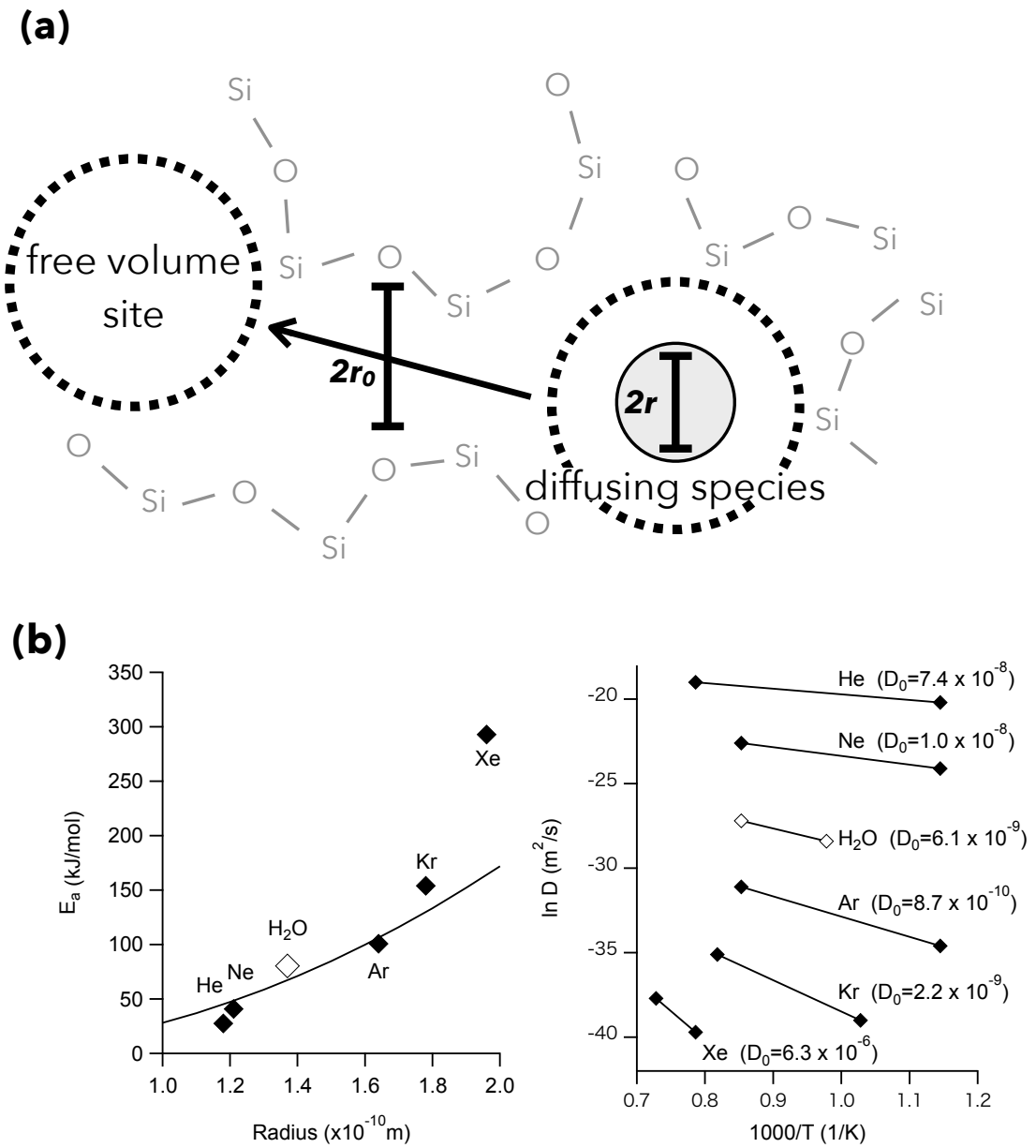


**Figure 4**